



Published in final edited form as:

Nat Neurosci. 2013 July ; 16(7): 851–855. doi:10.1038/nn.3412.

Exome sequencing to identify *de novo* mutations in sporadic ALS trios

Alessandra Chesi^{1,11}, Brett T. Staahl², Ana Jovicic¹, Julien Couthouis¹, Maria Fasolino³, Alya R. Raphael¹, Tomohiro Yamazaki⁴, Laura Elias², Meraida Polak⁵, Crystal Kelly⁵, Kelly L. Williams^{6,7,8}, Jennifer A. Fifita^{6,8}, Nicholas J. Maragakis⁹, Garth A. Nicholson^{6,7}, Oliver D. King¹⁰, Robin Reed⁴, Gerald R. Crabtree², Ian P. Blair^{6,7,8}, Jonathan D. Glass⁵, and Aaron D. Gitler^{1,11}

¹Department of Genetics, Stanford University School of Medicine, Stanford, CA 94305

²Howard Hughes Medical Institute and Department of Developmental Biology, Stanford University School of Medicine, Stanford, CA 94305

³Neuroscience Graduate Group, Perelman School of Medicine at the University of Pennsylvania, Philadelphia, PA 19104

⁴Department of Cell Biology, Harvard Medical School, Boston, MA 02115

⁵Department of Neurology, Emory University, Atlanta, GA 30322

⁶Northcott Neuroscience Laboratory, ANZAC Research Institute, Sydney, NSW, 2139, Australia

⁷Sydney Medical School, University of Sydney, Sydney, NSW, 2006, Australia

⁸Australian School of Advanced Medicine, Macquarie University, Sydney, NSW 2109, Australia

⁹Department of Neurology, Johns Hopkins University School of Medicine, Baltimore, MD 21205

¹⁰Department of Cell and Developmental Biology, University of Massachusetts Medical School, Worcester, MA 01655

Abstract

ALS is a devastating neurodegenerative disease whose causes are still poorly understood. To identify additional genetic risk factors, here we assess the role of *de novo* mutations in ALS by sequencing the exomes of 47 ALS patients and both of their unaffected parents (n=141 exomes).

Users may view, print, copy, download and text and data- mine the content in such documents, for the purposes of academic research, subject always to the full Conditions of use: http://www.nature.com/authors/editorial_policies/license.html#terms

¹¹Correspondence should be addressed to: Aaron D. Gitler 300, Pasteur Drive, M322 Alway Building, Stanford, CA 94305, 650-725-6991 (phone), agitler@stanford.edu. Alessandra Chesi, 300 Pasteur Drive, M322 Alway Building, Stanford, CA 94305, 650-725-6991 (phone), chesi@stanford.edu.

Author Contributions

A.C. performed all of the exome sequencing and analysis. B.T.S. and A.J. performed the primary neuron experiments. B.T.S. performed co-immunoprecipitation experiments with direction from G.R.C. J.C., M.F., and A.R.R. performed Sanger sequencing and helped A.C. with exome sequencing. T.Y. and R.R. performed SS18L1/FUS physical association experiments. L.E. performed mass spectrometry analysis. N.J.M. and J.D.G. contributed ALS patient samples, with assistance from M.P. and C.K., and helped design experiments. K.L.W. J.A.F., G.A.N., and I.P.B. contributed ALS patient samples and performed experiments to identify SS18L1 variant in Australian FALS pedigree. O.D.K. performed prion-like domain analysis for SS18L1 and SS18. A.D.G. and A.C. wrote the manuscript with input from all authors.

We found that amino acid-altering *de novo* mutations are enriched in genes encoding chromatin regulators, including the neuronal chromatin remodeling complex component *SS18L1/CREST*. *CREST* mutations inhibit activity-dependent neurite outgrowth in primary neurons, and *CREST* associates with the ALS protein *FUS*. These findings expand our understanding of the ALS genetic landscape and provide a resource for future studies into the pathogenic mechanisms contributing to sporadic ALS.

Amyotrophic lateral sclerosis (ALS), also known as Lou Gehrig's disease, is a fatal adult-onset neurodegenerative disease characterized by loss of motor neurons¹. Although ~10% of cases have a family history of ALS (FALS), the majority of cases are sporadic (SALS). There have been several recent advances in defining the genetic landscape of FALS. These include discoveries of mutations in *TARDBP*, *FUS*, *VCP*, *OPTN*, *UBQLN2*, *C9orf72*, and *PFN1* as new FALS disease genes²⁻⁸. Together with mutations in *SOD1*⁹, the causes of two thirds of FALS cases have now been elucidated. There have also been significant inroads into understanding SALS etiology and now genetic contributors for ~11% of SALS cases are known. Since it is likely that genetics plays a central role in this form of the disease, there is intense interest in defining additional genetic causes and risk factors for SALS.

A possible genetic mechanism for sporadic disease is *de novo* mutation – a mutation that arises spontaneously in the germline of one of the unaffected parents. Indeed, *de novo* mutations have recently been identified as contributors to neurodevelopmental disorders such as autism spectrum disorders, schizophrenia, and mental retardation¹⁰⁻¹⁶. There have been confirmed *de novo* mutations in known ALS genes in apparently sporadic ALS cases¹⁷⁻¹⁹, indicating that, in principle, this mechanism could also contribute to ALS.

Results

To test the hypothesis that *de novo* mutations contribute to risk for ALS, we performed a systematic analysis of ALS trios (ALS patient and both unaffected parents, Fig. 1a). Because ALS is a late onset disease, trios for which DNA samples are available for patients and their parents are much rarer than for early onset ones like autism. Nevertheless, we were able to assemble a collection of 47 ALS trios and we performed whole exome sequencing on all 141 individuals ($47 \times 3 = 141$ exomes). We pre-screened all 47 ALS cases for the *C9orf72* hexanucleotide repeat expansion^{20, 21} and they were all negative. See Supplementary Table S1 for clinical and demographic information.

We achieved an average coverage of 56X across all samples, and on average 87% of the target bases in each individual were covered by at least 10 independent sequence reads (Supplementary Table S2). Following validation by Sanger sequencing we identified 25 novel *de novo* amino acid-altering variants (non-synonymous, NS): 20 missense, 1 nonsense, 1 splicing, 2 frameshift and 1 in-frame deletion. The observed *de novo* mutation rate is consistent with those reported in recent studies of autism spectrum disorders¹⁰⁻¹³ and see Supplementary Table S3). The frequency distribution of *de novo* NS mutations closely followed a Poisson distribution, indicating that multiple *de novo* events within a single individual do not contribute to ALS risk (Supplementary Fig. S1).

Table 1 shows the list of 25 novel *de novo* NS mutations identified in the 47 ALS trios. We first asked if there are any functional categories or cellular pathways enriched in this list. Functional annotation analysis performed with DAVID (v6.7)²² revealed a significant enrichment of genes encoding chromatin regulators (5 out of 25: EHMT1, FOXA1, HDAC10, SRCAP, and SS18L1 (see below and Staahl et al submitted); $P=1\times 10^{-2}$; corrected for the multiple pathways that were tested). Are *de novo* mutations simply more common in chromatin regulator genes or is this enrichment in our ALS list meaningful? To address this question, we sought a “control” set of trios. The recent analysis of *de novo* mutations in autism spectrum disorders included some exome data on unaffected siblings¹⁰. We used the *de novo* mutations found in unaffected siblings (n=50) to perform the same functional analysis. This list of *de novo* mutations was not enriched for any functional category (Supplemental Fig. S2), supporting the idea that chromatin regulator genes and defects in chromatin regulation could contribute to ALS. Indeed, drugs modulating histone acetylation have shown protective effects in ALS mouse models and patient iPSC-derived motor neurons^{23–25} and have undergone phase 2 clinical studies in ALS subjects²⁶. Our results now reveal potential genetic connections to ALS as well.

Three genes on the list have been implicated in neurite outgrowth (NTM, VCL, SS18L1)^{27–31}. Defects in neurite outgrowth have been seen in zebrafish models of ALS³² and in iPSC-derived motor neurons from ALS patients²⁵. One of these genes, *SS18L1* (also called *CREST*), is expressed only in post mitotic neurons and we have found encodes an essential subunit of a neuron-specific chromatin-remodeling complex (nBAF) (Staahl et al in press) that resembles yeast SWI/SNF and SWR and is also called mSWI/SNF³³. nBAF controls activity-induced dendrite outgrowth^{29, 31} and is strongly expressed in the brain and spinal cord, where it localizes to the nucleus (Fig. 1c). *CREST* is a calcium-regulated transcriptional activator, a property that requires the last 9 amino acids of *CREST*, which is reported to interact with the histone acetylase CBP (Fig. 1b and²⁹). Remarkably, we identified a *de novo* mutation in *SS18L1/CREST* that introduces a stop codon removing the exact same last nine amino acids (p.Q388stop, Table 1 and Fig. 1b).

To determine the functional significance of this mutation in neurons, we tested its effects in primary cortical neurons isolated from mouse embryos. Depolarizing these primary neuronal cultures with KCl induced dramatic dendrite outgrowth (Fig. 1d), increasing the total dendrite length (Fig. 1e) and number of dendritic branch points per neuron (Fig. 1f). We transfected these neurons with GFP, WT *CREST* or a mutant *CREST* lacking the last 9 amino acids (*CREST*_{1–393}; this truncation in the mouse *CREST* homolog corresponds to *CREST*_{1–388} in human *CREST*, Fig. 1b). Expression of GFP or WT *CREST* had no effect on KCl-induced dendrite outgrowth (Fig. 1 d–f), whereas the presence of mutant *CREST* profoundly inhibited dendrite outgrowth (Fig. 1 d,e) and markedly decreased complexity of the dendritic arbors (Fig. 1f). These functional studies in primary neurons indicate that this mutation is likely deleterious and its dominant negative properties are consistent with a heterozygous mutation being able to cause disease.

To further examine a genetic role for *SS18L1* in ALS, we analyzed exome sequence data from index cases of 62 ALS families that were negative for all known ALS genes including *C9orf72*. In one case (individual III:2, family ALS296, Fig. 2a), we identified a novel

missense mutation (p.I123M) that was absent from public SNP and exome databases. We also performed targeted SNP genotyping on 693 control individuals from the same population and this variant was absent. Re-sequencing in this family showed the p.I123M variant was absent from the unaffected parent of this index case, implying segregation of the mutation from the affected (deceased) parent (Fig. 2a). To test the functional significance of this variant and to extend our studies to a cell type more clinically relevant to ALS, we tested its effects in cultures of primary motor neurons isolated from mouse embryos. We transfected motor neurons with GFP, WT CREST or the two mutants (CREST₁₋₃₉₃ or CREST_{I123M}). Strikingly, compared to GFP or WT CREST, expression of the mutants CREST₁₋₃₉₃ or CREST_{I123M} significantly blocked depolarization-induced dendrite outgrowth (Fig. 2b) and the increase in dendritic arbor complexity (Fig. 2c). Thus, these functional experiments in primary motor neurons provide evidence to support the pathogenicity of the two CREST variants identified in ALS patients.

The defects in dendritic morphology elicited by the two SS18L1/CREST mutant proteins in our primary neuron experiments are strikingly reminiscent of dendrite patterning defects observed in neurons cultured from FUS-deficient mice³⁴. We therefore considered the possibility that FUS and SS18L1 might physically associate. We (GRC and LE) conducted mass spectrometry studies of nBAF complexes affinity purified at low stringency (150 mM NaCl, 0.1% NP-40, 50mM Tris-HCL, pH 8.0) from P1 cortical neurons for proteins that interact with nBAF in cortical neurons. We detected 81 peptides from FUS representing 29.6 % coverage in these mass spectrometry studies. To further explore the potential physical interaction of FUS and CREST, we performed immunoprecipitation assays from nuclear extracts isolated from P1 mouse cortical neurons. Immunoprecipitating endogenous CREST from these extracts followed by immunoblotting with a FUS antibody demonstrated that CREST and FUS interact in neurons (Fig. 2d). We noted the interaction between CREST and FUS, when using the reciprocal immunoprecipitation (FUS antibody for IP, SS18L1/CREST antibody for immunoblot), was nearly undetectable. This could be indicative of different relative abundances. FUS might be more abundant than CREST and therefore we detect the interaction only one way. Another possibility is that the FUS antibody masks the binding site of CREST on FUS. To address this we performed quantitative western blots to determine the amounts of FUS and Brg (the core ATPase was used as a representative of the nBAF complexes of which CREST is a core subunit) per cell. We estimate there to be 3×10^5 molecules of BRG and 1.2×10^6 molecules of FUS per cell (data not shown). Therefore, FUS is at least 4-fold more abundant, and not a core BAF complex component, but perhaps transiently associates with CREST perhaps in a regulatory role. Because CREST is a dedicated subunit of the nBAF complex in neurons we wondered if using antibodies against other nBAF subunits would immunoprecipitate FUS. Indeed, we find many of the BAF subunits co-immunoprecipitate FUS (Figure 2e). Interestingly, Polybromo, which is a PBAF complex subunit and does not contain CREST, co-immunoprecipitated FUS. Therefore, FUS must be binding to a surface on the BAF complex other than CREST. This surface might be on Brg or BAF57 as these IPs co-immunoprecipitated FUS the weakest and therefore the antibodies to these subunits could be blocking the nBAF-FUS interaction. Together, these experiments provide evidence that CREST and the nBAF chromatin remodelling complex can associate with FUS in neurons.

Intriguingly, bioinformatics analysis revealed the presence of predicted prion-like domains in SS18L1 and SS18 (Fig. S3). These domains are present in an expanding class of neurodegenerative disease proteins, including TDP-43, FUS, TAF15, EWSR1, hnRNPA2B1, and hnRNPA1, and are able to drive aggregation of these proteins^{35–40}. In the future, it will be important to define how SS18L1's prion-like domain contributes to its normal function and if it facilitates co-aggregation with FUS or other aggregation-prone RNA-binding proteins in disease. Together, these data support a potential role of the identified SS18L1/CREST variants in ALS and implicate additional nBAF complex components as candidates for further investigation in the disease.

Discussion

We have sequenced the exomes of 47 ALS trios. These results provide a systematic analysis of *de novo* mutations in ALS and reveal genes encoding chromatin regulators as new candidates for ALS genetic contributors. Notably, in addition to SS18L1, we identified a *de novo* truncating mutation in *SRCAP* in another ALS trio (Table 1). Like SS18L1/CREST, *SRCAP* is also a CBP-interacting transcriptional co-activator⁴¹, further underscoring a potential role of CBP-associated chromatin regulators in ALS. Indeed, FUS itself is a key transcriptional regulator via interactions with CBP⁴². Mutations in 8 of 15 subunits of BAF complexes have been identified as causative in Coffin-Siris, a rare congenital anomaly syndrome characterized by growth deficiency, intellectual disability, microcephaly, coarse facial features and hypoplastic nail of the fifth finger and/or toe^{43,44}, and Nicolaides-Baraitser Syndromes, which includes features of intellectual disability with marked language impairment, microcephaly, epilepsy and morphological defects^{45,46} and have also been found in sporadic autism¹⁰ and intellectual disability⁴⁷ as well as schizophrenia⁴⁸. It is tempting to speculate about possible pathophysiological connections between neurodevelopmental and neurodegenerative disorders⁴⁹.

Beyond the chromatin regulator genes, the identification of a *de novo* mutation in the type XIX collagen gene *COL19A1* is intriguing because the expression of this molecule has been recently shown to be markedly upregulated in the muscle at end-stage of disease in a mouse model of inherited ALS (*SOD1*^{G39A}) and *Coll19a1* expression negatively correlates with survival⁵⁰. Future studies will be required to define the effect of this variant on *COL19A1* expression and the effect it has on muscle function during disease progression.

Additional functional studies in cell culture and animal models as well as re-sequencing these genes in larger ALS patient populations will be needed to assess the pathogenicity of the genes identified in this study. We propose that the specific genes we identify here, as well as their network of interacting partners (genetic and physical interactions), especially the other components of the SS18L1/CREST-containing nBAF chromatin remodeling complex are now candidates for evaluation in larger ALS patient cohorts. Using the autism exome sequencing efforts as a guide^{10–13}, we anticipate that increasing the number of ALS trios analyzed, integrating data from multiple studies, and focusing on key nodes in protein interaction networks will help strengthen and focus disease gene discovery efforts. Finally, this approach could be applied broadly to other neurodegenerative diseases, such as Parkinson disease and Alzheimer disease.

Online Methods

ALS trios

Details of the ALS patients used in this study are compiled in Table S1. Genomic DNA from human ALS patients and both of their unaffected parents was collected at Emory University School of Medicine (IRB# IRB-133-98) and the Johns Hopkins University School of Medicine. ALS samples were verified to meet El Escorial criteria for definite or probable ALS.

Exome capture, alignments and base-calling

Exomes for the 47 trios were captured with Agilent SureSelect Human All Exon 50Mb. Libraries were indexed, pooled and sequenced on Illumina HiSeq2000 machines (paired-end, 100-bp reads, 5 or 6 libraries per lane). Reads were mapped to a custom GRCh37/hg19 build using BWA 0.5.9⁵¹. Picard-tools 1.55 was used to flag duplicate reads (<http://picard.sourceforge.net/>). GATK (v1.3-2-gcdd40d1)⁵² IndelRealigner was used to realign reads around insertion/deletion (indel) sites. Read qualities were recalibrated using GATK Table Recalibration. Genotypes were generated simultaneously for all samples with GATK Unified Genotyper. Variant quality score recalibration was performed on SNPs calls (using HapMap v3.3 and the Omni chip array from the 1000 Genomes Project as training data) and calls were filtered at 99.0 truth sensitivity level⁵³. Raw indel calls were filtered using FILTER= "QD < 2.0 || ReadPosRankSum < -20.0 || InbreedingCoeff < -0.8 || FS > 200.0". Predicted *de novo* events were identified as sites where both parents were homozygous for the reference sequence and the offspring was heterozygous. Paternity and maternity was verified by checking the percentage of shared heterozygous mutations between child and mother or father in each trio (~50%). To identify rare private variants (novel), the full variant list was compared against dbSNPv135, the NHLBI Exome Sequencing Project (ESP 5400) and the 1000 Genomes Project (Feb 2012). Annotation was performed using ANNOVAR (<http://www.openbioinformatics.org/annovar>).

Sanger sequencing validation of variants

All amino acid-altering *de novo* novel events were validated by designing primers with Primer3 (v.2.3.0) followed by PCR amplification and Sanger sequencing of father, mother and proband DNA samples.

Functional enrichment analysis

Functional enrichment analysis was performed with the Functional Annotation Chart tool of DAVID v. 6.7⁵⁴ using the human genome as background. P-values were calculated using a modified Fisher Exact Test⁵⁵ and corrected using Bonferroni correction for multiple comparisons.

Sequence analysis of Familial ALS cases

Index cases from 62 ALS families were recruited through neurogenetic clinics at Concord Hospital, Sydney, as well as at the Molecular Medicine Laboratory, Concord Hospital, a referral centre for ALS DNA diagnostic testing. Most families were of European descent.

DNA samples from 693 control individuals were obtained from the Australian MND DNA Bank. Patients and family members provided informed written consent regulated by the Human Research Ethics Committee of the Sydney South West Area Health Service. All families had previously been screened for mutations in known ALS genes including *C9ORF72*, *TARDBP*, *SOD1*, *FUS*, *PFN1*, *OPTN*, *VCP*, *UBQLN2*, *ANG*, *FIG4*, *DCTN1*, and *CHMP2B*.

Exomes for familial cases were captured with Illumina TruSeq Exome Enrichment kit. Libraries were indexed, pooled and sequenced on Illumina HiSeq2000 instruments (paired-end, 100-bp reads, 6 libraries per lane). Reads were mapped to the human genome (hg19, Genome Reference Consortium Human Build 37) using BWA.

Clinical and demographic data

Family ALS296 was of UK ancestry. The index case (individual III:2, Fig. 2a) was diagnosed with bulbar onset ALS at 35 years, disease duration of 1 year. The father of this index case (individual II:2, Fig. 2a) was diagnosed with bulbar onset ALS at 48 years, disease duration of 1 year. Individual II:1 (Fig. 2a) was diagnosed with limb onset ALS and died at 61 years.

Immunohistochemistry

Formalin-fixed, paraffin-embedded human spinal cord sections, obtained from the University of Pennsylvania Center for Neurodegenerative Disease Research Brain Bank, were rehydrated and subjected to Antigen Retrieval with Citrate Buffer pH 6.0 (Vector Labs). After washing with 0.1% PBS-Tween blocking was performed with 2% BSA, 5% NGS, 0.1% PBS-T for 60 minutes at 25°C. Sections were incubated with Rabbit anti-CREST (1:50; Proteintech) in 0.1% PBST overnight at 4°C. After washing with 0.1% PBST, sections were incubated with Goat anti-Rabbit-568 IgG (1:500; Invitrogen) for 2 hour at 25°C. Sections were then incubated DAPI, washed with PBS and mounted with 4% *n*-Propyl gallate (Sigma) in 90% glycerol, 10% phosphate buffered saline (PBS).

Mouse primary neuron culture and transfection

All mouse experiments were performed in compliance with institutional guidelines and regulations. E18.5 cortical neurons were isolated using the MACSTM neuron isolation kit. Motor neurons were isolated from E12.5 mouse spinal cord using Papain Dissociation System (Worthington). Dissociated cells were transfected with GFP or other constructs using Nucleofector (Amaxa shuttle) before plating on poly-L-ornithine, Laminin and fibronectin coated coverslips. Cortical neuron culture media contained DMEM/F12 with putrescine, 2-mercaptoethanol, transferrin, insulin, selenium, progesterone, MEM vitamin additive and 5% FBS. Motor neuron culture media contained Neurobasal supplemented with B27 (Invitrogen), 2% horse serum, L-glutamine (0.5 mM), L-glutamate (25 µM), BDNF (1 ng/ml), GDNF (100 pg/ml) and CNTF (10 ng/ml).

Dendrite outgrowth assay

CREST, *CREST*₁₋₃₉₃, or *CREST*_{I123M} were cloned into the pCIG-IRES-*eGFP* plasmid. 50ng of the respective plasmids mixed with 450ng pCIG-IRES-*eGFP* plasmid was transfected

into 250,000 dissociated E18.5 mouse cortical neurons or E12.5 mouse motor neurons using Nucleofector (AMAXA shuttle) and plated onto coated coverslips. The neural cultures were grown for 6 days, +/- 30mM KCl for the last day. To define dendrite structure, cultures were fixed with 4% PFA and stained with anti-GFP (Molecular Probes) and anti-MAP2 (Sigma) and Alexa-Fluor-488, -568 (Invitrogen) secondary antibodies (1:1000) and DAPI and mounted as described above. Pictures of GFP+/MAP2+ neurons were taken with a Leica DM5000 fluorescent microscope. Dendrite analysis was done with ImageJ and NeuronJ software.

Co-immunoprecipitation

For co-IPs, antibodies against FUS (A300-293A), BAF250B (A301-046A), Polybromo (A301-590A), BAF57 (A300-810A), BAF170 (A301-039A) all from Bethyl, CREST (H-80) from Proteintech, Brg (G7 or H88), BAF250A (H90x) all from Santa Cruz, BAF60c and BAF45c, BAF155-3 from the Crabtree lab were used. Rabbit or mouse IgG antibodies from Santa Cruz were used as a control. P1 mouse cortices were isolated using standard procedures. Nuclear extracts were prepared and incubated with respective antibodies and Protein A or G dynabeads overnight and washed 6 times in PBS/0.1% Triton X-100 as described in ⁵⁶. Western blots were probed with antibodies to Fus (ab23439) from Abcam, Brg (G7) and CREST (M15) from Santa Cruz. LiCor secondary antibodies were used for detection.

Statistical Analysis

For the functional enrichment analysis in ALS and control trios we used the Functional Annotation Chart tool of DAVID v. 6.7 ⁵⁴ with the human genome as background. P-values were calculated using a modified Fisher Exact Test ⁵⁵ and corrected using Bonferroni correction for multiple comparisons. For the primary neuronal culture assays we used the unpaired two-sided Student's t-test. The number of biologically independent experiments and P-values are indicated in the figure legends. The sample sizes were chosen according to standard practice in the field.

Supplementary Material

Refer to Web version on PubMed Central for supplementary material.

Acknowledgments

This work was supported by NIH Director's New Innovator Award 1DP2OD004417 (A.D.G.), NIH grants 1R01NS065317 (A.D.G.) and 5U01NS062713 (N.J.M.), and the Department of Defense ALS Research Program (N.J.M.). A.D.G. is a member of the Biogen Idec ALS genome sequencing consortium. A.D.G. is a Pew Scholar in the Biomedical Sciences, supported by The Pew Charitable Trusts, and a Rita Allen Foundation Scholar. A.D.G. and J.D.G. are supported by the Packard Center for ALS Research at Johns Hopkins. In Australia the work was supported by the National Health and Medical Research Council of Australia (1004670, 511941) and the Motor Neurone Disease Research Institute of Australia.

References

1. Andersen PM, Al-Chalabi A. *Nat Rev Neurol*. 2011; 7:603–615. [PubMed: 21989245]
2. Sreedharan J, et al. *Science*. 2008; 319:1668–1672. [PubMed: 18309045]

3. Vance C, et al. *Science*. 2009; 323:1208–1211. [PubMed: 19251628]
4. Kwiatkowski TJ, et al. *Science*. 2009; 323:1205–1208. [PubMed: 19251627]
5. Johnson JO, et al. *Neuron*. 2010; 68:857–864. [PubMed: 21145000]
6. Maruyama H, et al. *Nature*. 2010; 465:223–226. [PubMed: 20428114]
7. Deng HX, et al. *Nature*. 2011; 477:211–215. [PubMed: 21857683]
8. Wu CH, et al. *Nature*. 2012
9. Rosen D, et al. *Nature*. 1993; 362:59–62. [PubMed: 8446170]
10. O’Roak BJ, et al. *Nature*. 2012; 485:246–250. [PubMed: 22495309]
11. Neale BM, et al. *Nature*. 2012; 485:242–245. [PubMed: 22495311]
12. Sanders SJ, et al. *Nature*. 2012; 485:237–241. [PubMed: 22495306]
13. Iossifov I, et al. *Neuron*. 2012; 74:285–299. [PubMed: 22542183]
14. Xu B, et al. *Nat Genet*. 2011; 43:864–868. [PubMed: 21822266]
15. Girard SL, et al. *Nat Genet*. 2011; 43:860–863. [PubMed: 21743468]
16. Vissers LE, et al. *Nat Genet*. 2010; 42:1109–1112. [PubMed: 21076407]
17. Alexander MD, et al. *Ann Neurol*. 2002; 52:680–683. [PubMed: 12402272]
18. Chio A, et al. *Neurobiol Aging*. 2011; 32:553 e523–556 . [PubMed: 20598774]
19. DeJesus-Hernandez M, et al. *Hum Mutat*. 2010
20. DeJesus-Hernandez M, et al. *Neuron*. 2011; 72:245–256. [PubMed: 21944778]
21. Renton AE, et al. *Neuron*. 2011; 72:257–268. [PubMed: 21944779]
22. Huangda W, et al. *Curr Protoc Bioinformatics*. 2009; Chapter 13(Unit 13):11.
23. Ryu H, et al. *J Neurochem*. 2005; 93:1087–1098. [PubMed: 15934930]
24. Rouaux C, et al. *J Neurosci*. 2007; 27:5535–5545. [PubMed: 17522299]
25. Egawa N, et al. *Sci Transl Med*. 2012; 4:145ra104 .
26. Cudkowicz ME, et al. *Amyotroph Lateral Scler*. 2009; 10:99–106. [PubMed: 18688762]
27. Gil OD, Zanazzi G, Struyk AF, Salzer JL. *J Neurosci*. 1998; 18:9312–9325. [PubMed: 9801370]
28. van Horck FP, Lavazais E, Eickholt BJ, Moolenaar WH, Divecha N. *Curr Biol*. 2002; 12:241–245. [PubMed: 11839279]
29. Aizawa H, et al. *Science*. 2004; 303:197–202. [PubMed: 14716005]
30. Qiu Z, Ghosh A. *Neuron*. 2008; 60:775–787. [PubMed: 19081374]
31. Wu JI, et al. *Neuron*. 2007; 56:94–108. [PubMed: 17920018]
32. Kabashi E, et al. *Hum Mol Genet*. 2010; 19:671–683. [PubMed: 19959528]
33. Khavari PA, Peterson CL, Tamkun JW, Mendel DB, Crabtree GR. *Nature*. 1993; 366:170–174. [PubMed: 8232556]
34. Fujii R, et al. *Curr Biol*. 2005; 15:587–593. [PubMed: 15797031]
35. Cushman M, Johnson BS, King OD, Gitler AD, Shorter J. *J Cell Sci*. 2010; 123:1191–1201. [PubMed: 20356930]
36. Gitler AD, Shorter J. *Prion*. 2011; 5:179–187. [PubMed: 21847013]
37. King OD, Gitler AD, Shorter J. *Brain Res*. 2012; 1462:61–80. [PubMed: 22445064]
38. Couthouis J, et al. *Proc Natl Acad Sci U S A*. 2011; 108:20881–20890. [PubMed: 22065782]
39. Couthouis J, et al. *Hum Mol Genet*. 2012; 21:2899–2911. [PubMed: 22454397]
40. Kim HJ, et al. *Nature*. 2013; 495:467–473. [PubMed: 23455423]
41. Monroy MA, et al. *J Biol Chem*. 2001; 276:40721–40726. [PubMed: 11522779]
42. Wang X, et al. *Nature*. 2008; 454:126–130. [PubMed: 18509338]
43. Bultman S, et al. *Mol Cell*. 2000; 6:1287–1295. [PubMed: 11163203]
44. Tsurusaki Y, et al. *Nat Genet*. 2012; 44:376–378. [PubMed: 22426308]
45. Wolff D, et al. *Mol Syndromol*. 2012; 2:237–244. [PubMed: 22822383]
46. Van Houdt JK, et al. *Nat Genet*. 2012; 44:445–449. S441 . [PubMed: 22366787]
47. Hoyer J, et al. *Am J Hum Genet*. 2012; 90:565–572. [PubMed: 22405089]
48. Loe-Mie Y, et al. *Hum Mol Genet*. 2010; 19:2841–2857. [PubMed: 20457675]

49. Lule D, Ludolph AC, Ludolph AG. *Med Hypotheses*. 2008; 70:1133–1138. [PubMed: 18158219]
50. Majounie E, et al. *Lancet Neurol*. 2012; 11:323–330. [PubMed: 22406228]
51. Li H, Durbin R. *Bioinformatics*. 2009; 25:1754–1760. [PubMed: 19451168]
52. McKenna A, et al. *Genome Res*. 2010; 20:1297–1303. [PubMed: 20644199]
53. DePristo MA, et al. *Nat Genet*. 2011; 43:491–498. [PubMed: 21478889]
54. Huang da W, Sherman BT, Lempicki RA. *Nat Protoc*. 2009; 4:44–57. [PubMed: 19131956]
55. Hosack DA, Dennis G Jr, Sherman BT, Lane HC, Lempicki RA. *Genome Biol*. 2003; 4:R70. [PubMed: 14519205]
56. Dufu K, et al. *Genes Dev*. 2010; 24:2043–2053. [PubMed: 20844015]

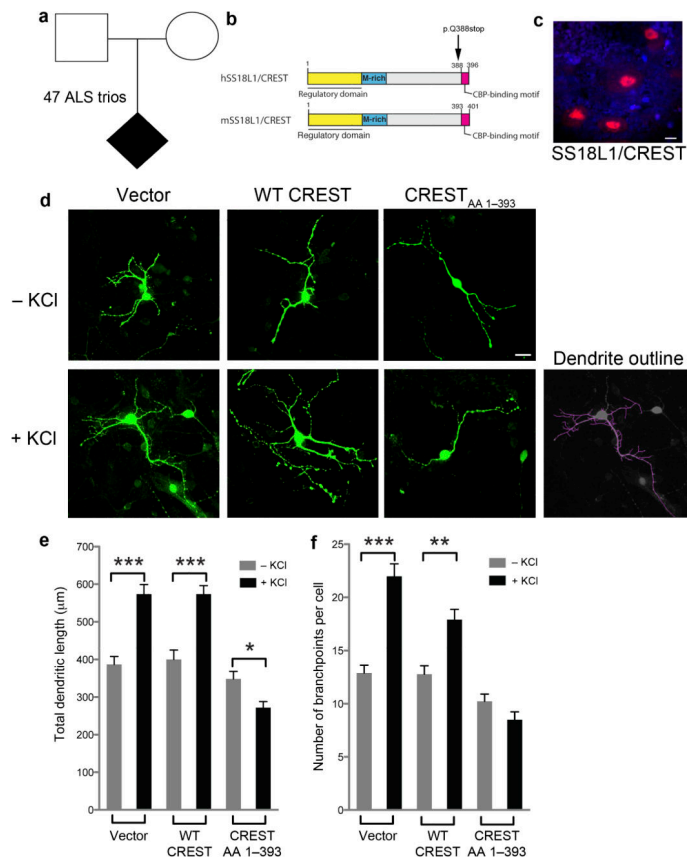


Figure 1.

The SS18L1/CREST *de novo* mutation (Q388stop) identified in an ALS trio inhibits activity-dependent dendritic outgrowth. **a)** We sequenced the exomes of 47 ALS patients and both unaffected parents ($n = 141$ exomes) to identify *de novo* mutations. **b)** We identified a *de novo* mutation in the neuronal chromatin remodeling complex subunit SS18L1/CREST, which introduces a premature termination codon, deleting the CBP-binding motif contained within the last nine amino acids. h=human; m=mouse. **c)** SS18L1/CREST is expressed in motor neurons of the adult spinal cord and localizes to the nucleus (arrow). Scale bar 10 μm . **d)** Functional validation of the CREST *de novo* mutation in primary neurons. Primary cortical neurons were isolated from E18.5 mouse embryos, transfected with Vector-IRES-GFP, CREST-IRES-GFP or CREST_{AA 1-393}-IRES-GFP (The 1-393 truncation of mouse CREST corresponds to 1-388 of human CREST, which we identified in the ALS trio as Q388stop). Neurons were cultured for 5 days and stimulated overnight with 30mM KCl where indicated. Control vector and CREST overexpression do not affect dendrite outgrowth in response to KCl depolarization. CREST_{AA 1-393} significantly reduces total dendrite length in response to KCl depolarization. An example of the dendrite outline tracing used to quantify dendritic length and number of branch points is shown. Scale bar 10 μm . **e)** The average values are from three independent experiments, each with three coverslips per condition with 15–20 GFP+ neurons scored per coverslip. **f)** # branch points per cell is affected in a similar fashion as total dendrite length. Error bars, S.E. * $P < 0.02$, ** $P < 0.002$, *** $P < 0.0005$, Student's t-test.

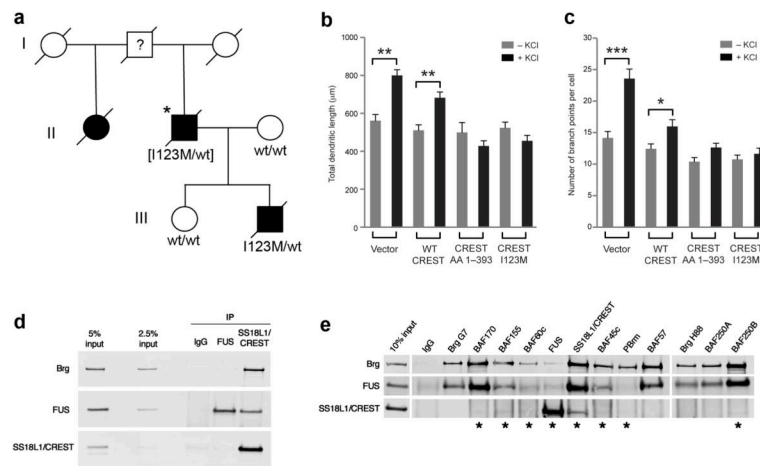


Figure 2. Identification of an additional *SS18L1*/CREST variant in FALS case and interaction with FUS. **a**) Novel *SS18L1* missense variant in familial ALS. Genotypes of available DNA samples for the indicated *SS18L1* variant are shown ('wt' denotes wild type, 'I123M' denotes mutant). The variant c.T369G (p.I123M) was identified in affected individual III:2 (the index case) and was absent in unaffected individuals II:3 and III:1. The genotype of sample II:2 (*) was inferred from the genotypes of spouse and progeny. The question mark (?) for individual I:2 indicates that no historical clinical notes were available. **b**) Motor neurons transfected with GFP or WT CREST respond to KCl stimulation by increasing the total dendritic length. Transfection of CREST₁₋₃₉₃ or CREST_{I123M} inhibits stimulation-induced dendrite outgrowth. The average values are from two independent experiments, each with four coverslips per condition with 30–35 GFP+ neurons scored per coverslip. **c**) # of branch points in motor neurons is affected in a similar fashion as total dendrite length. Error bars, S.E. *P<0.02, **P<0.002, ***P<0.0005, Student's t-test. **d,e**) FUS and SS18L1/CREST can physically associate in mouse cortical neurons. **d**) As a positive control, nBAF complex core subunit Brg, was co-immunoprecipitated by SS18L1/CREST. The SS18L1/CREST antibody also co-immunoprecipitated FUS. **e**) Antibodies against several other nBAF subunits co-immunoprecipitate FUS. * FUS band is visible.

Table 1

List of novel amino acid-altering *de novo* variants identified in 47 ALS trios.

Trio #	Genomic coordinates (hg19)	Nucleotide change	Gene	Description	Amino acid change
19	chr1:26672011	C/A	AIM1L	absent in melanoma 1-like protein	p.Gly380Tyr
44	chr3:138219345	T/G	CEP70	centrosomal protein 70kDa	p.Asp478Ala
3	chr11:62677899	A/G	CHRM1	cholinergic receptor, muscarinic	p.Leu225Pro
37	chr16:58555162	A/G	CNOT1	CCR4-NOT transcription complex, subunit 1	p.Phe2326Ser
12	chr6:70672763	G/C	COL19A1	collagen, type XIX, alpha 1	splicing
33	chr5:122909210	A/-	CSNK1G3	casein kinase	Frameshift indel
37	chr9:140611221	G/A	EHMT1	euchromatic histone-lysine N-methyltransferase	p.Ala77Thr
23	chr19:18561734	G/A	ELL	elongation factor RNA polymerase II	p.Arg340Tyr
18	chr14:38061661	GCTCAGCGCCGTACCCATGGCCGTAC/-	FOXA1	transcriptional activator of the forkhead class of DNA-binding proteins	Non-frameshift indel
20	chr7:4800826	G/A	FOXP1	transcriptional activator of the forkhead class of DNA-binding proteins	p.Val610Met
33	chr14:105518381	C/G	GPR132	G protein-coupled receptor	p.Lys31Asn
23	chr22:50688552	C/T	HDAC10	histone deacetylase	p.Gly110Glu
23	chr16:22826121	C/A	HS3ST2	heparan sulfate (glucosamine) 3-O-sulfotransferase	p.Gln64Lys
50	chr6:17850560	C/G	KIF13A	kinesin family member	p.Gln237His
3	chr11:132016267	C/T	NTM	(lg) domain-containing GPI-anchored cell adhesion molecule	p.Arg87Cys
48	chr15:65157668	C/G	PLEKHO2	pleckstrin homology domain containing protein	p.Pro302Ala
44	chr8:10466776	C/T	RP1L1	retinitis pigmentosa 1-like 1	p.Arg1611Gln
35	chr16:30740326	G/-	SRCAP	ATPase component of the chromatin-remodeling SRCAP complex	Frameshift indel
43	chr20:60749698	C/T	SS18L1	synovial sarcoma translocation gene on chromosome 18-like 1, component of neuron-specific nBAF chromatin remodeling complex	p.Gln388Stop
41	chr13:33703370	G/T	STARD13	STAR-related lipid transfer (START) domain containing protein	p.Leu364Ile
8	chr17:30202275	G/C	UTP6	small subunit (SSU) processome component	p.Ala428Gly
29	chr10:75865064	C/T	VCL	cytoskeletal protein associated with cell-cell and cell-matrix junctions	p.Pro796Leu
26	chr4:10117848	G/C	WDR1	WD repeat-containing protein	p.Phe9Leu
1	chr14:74371655	A/G	ZNF410	zinc finger protein	p.Tyr278Cys
43	chr16:89294680	G/A	ZNF778	zinc finger protein	p.Glu662Lys